

A Nanofiber-Based Gas Diffusion Layer for Improved Performance in Air Cathode Microbial Fuel Cells

*Original*

A Nanofiber-Based Gas Diffusion Layer for Improved Performance in Air Cathode Microbial Fuel Cells / Massaglia, Giulia; Serra, Tommaso; Pirri, Candido; Quaglio, Marzia. - In: NANOMATERIALS. - ISSN 2079-4991. - ELETTRONICO. - 13:20(2023), pp. 1-13. [10.3390/nano13202801]

*Availability:*

This version is available at: 11583/2983441 since: 2023-10-30T11:09:14Z

*Publisher:*

MDPI

*Published*

DOI:10.3390/nano13202801

*Terms of use:*

This article is made available under terms and conditions as specified in the corresponding bibliographic description in the repository

*Publisher copyright*

(Article begins on next page)



# Nanofiber-based gas diffusion layer for improve performance in Air-Cathode Microbial Fuel Cells

Giulia Massaglia <sup>1,2\*</sup>, Tommaso Serra<sup>1,2</sup>, Candido F. Pirri <sup>1,2</sup> and Marzia Quaglio <sup>1,2,\*</sup><sup>1</sup> Department of Applied Science and Technology, Politecnico of Turin, 10129, Corso Duca degli Abruzzi 29, Italy<sup>2</sup> Center for Sustainable Future and Technologies, Italian Institute of Technology, 10100, Via Livorno 60, Italy\* Correspondence: [giulia.massaglia@polito.it](mailto:giulia.massaglia@polito.it); [marzia.quaglio@polito.it](mailto:marzia.quaglio@polito.it)

## Abstract:

This work investigates a new nanostructured gas-diffusion-layer (nano-GDL) to improve performance of air-cathode Single-Chamber-Microbial-Fuel-Cells (a-SCMFCs). The new nano-GDLs improves the direct oxygen-reduction-reaction by exploiting the best of nanofibers from electrospinning in terms of high surface ratio to volume and high porosity, and laser-based processing to promote adhesion. Nano-GDLs by electrospinning were fabricated directly collecting two nanofibers mats on the same carbon-based electrode, acting as the substrate. Each layer was designed with a specific function: water resistant, oxygen permeable polyvinylidene-difluoride (PVDF) nanofibers served as a barrier to prevent water-based electrolyte leakage, while an inner layer of cellulose nanofibers was added to promote oxygen diffusion towards the catalytic sites. The maximum current density obtained for a-SCMFCs with the new nano-GDLs is  $(132.2 \pm 10.8) \text{ mA m}^{-2}$ , and it doubles the current density obtained with standard PTFE-based GDL ( $58.5 \pm 2.4 \text{ mA m}^{-2}$ ), used as reference material. The energy recovery (EF) factor, i.e. the ratio of the power output to the inner volume of the device, was then used to evaluate the overall performance of a-SCMFCs. a-SCMFCs with nano-GDL provided an EF value of  $60.83 \text{ mJ m}^{-3}$ : one order of magnitude higher than the value of  $3.92 \text{ mJ m}^{-3}$  obtained with standard GDL.

**Keywords:** Electrospinning; Fuel Cell; Laser-induced nanomaterials; Microbial Fuel Cells; Gas Diffusion Layer;; Triple phase boundary; Oxygen Reduction Reaction.

**Citation:** To be added by editorial staff during production.

Academic Editor: Firstname Last-name

Received: date

Revised: date

Accepted: date

Published: date



**Copyright:** © 2023 by the authors. Submitted for possible open access publication under the terms and conditions of the Creative Commons Attribution (CC BY) license (<https://creativecommons.org/licenses/by/4.0/>).

## 1. Introduction

The transition from carbon-based economies to sustainable human development, is boosting renewable energy systems [1]. Alongside the more traditional technologies for the valorization of renewable energy, like wind, solar, hydro-and geo-thermal and biomass, microbial fuel cells (MFCs) have gained great interest in recent years. MFCs are bio-electrochemical devices that combine a power production mechanism similar to that of traditional fuel cells, with biotechnological processes like water treatment [2-3], bioremediation [4], and sensing [5-7], thanks to the presence of electroactive bacteria at their **anodes** [8-12]. These microorganisms can directly transduce the chemical energy, entrapped into organic matter, into electrical energy. Indeed, electroactive bacteria work as anodic biocatalysts in anaerobic conditions, oxidizing organic matter dissolved into the electrolyte and releasing the produced electrons to the anode. Electrons flow continuously to the cathode compartment where their re-combination with terminal electron acceptors (TEAs) is ensured. MFCs in open-air configuration use oxygen as the TEA.

The target cathodic reaction is the direct oxygen reduction reaction (ORR). As demonstrated by several works in the literature [13-17], ORR is the usual choice for the cathodic reaction as oxygen maximizes power production while allowing environmental application of MFCs. Catalysts are needed to promote the ORR according to the direct reduction of O<sub>2</sub> in water and to optimize the reaction kinetics. If properly catalyzed, the secondary reaction pathway of the ORR, associated to the production of toxic hydrogen peroxide, can be completely avoided. The best performing catalyst is platinum [13-17]. Pt is applied at the surface of the cathode in such a way to ensure optimal contact with both the electrode itself and the electrolyte. The resulting interface is the most critical one for fuel cell technologies since it is associated to the triple-phase boundary, i.e. the zone where protons, electrons and oxygen molecules must reach the catalyst sites to react [18-21]. In this view the Gas Diffusion Layer (GDL) is a key component of fuel cells to manage diffusion of gaseous reactants, such as oxygen, to promote removal of excess water in proximity of the catalyst layer and, in MFCs, to minimize as much as possible the electrolyte leakage [22]. The ideal GDLs must satisfy several properties, such as high gas diffusion [23,24], good bending stiffness, continuous porosity, air permeability, water vapor diffusion, high surface area to volume ratio to ensure the water removal, good electrical and electronic conductivity to ensure the proper electrons' transfer and suitable mechanical stability [21]. For what concerns air-cathode single chamber microbial fuel cells (a-SCMFCs), commonly used GDLs are characterized by a backbone made of a carbon-based material acting as the electrode, which is then covered by the catalyst layer on one side [25], and by a hydrophobic coating, typically based on polytetrafluoroethylene (PTFE) on the side. PTFE is strongly hydrophobic and permeable to oxygen. These properties can be very useful to design GDLs for MFCs since this polymer can act as a barrier to avoid electrolyte leakage from the cell, while allowing oxygen diffusion, and contributing to avoid excess of water, so preventing the cathode flooding [26-30]. Nevertheless, the PTFE layer needs careful design in order to avoid any negative influence to the final behavior of the cathode. Guerrini et al. [30] demonstrated that excess PTFE in GDLs for open-air cathode MFCs, can make the electrode too hydrophobic preventing water from reaching the catalytic sites, **inhibiting the ORR** reaction. Moreover, many works in the literature, in the main fields of fuel cell technology, focused their attention on the GDLs' structure, that could be a bottleneck for improving of functionality of this layer [18-30]. Indeed, during last decades, nanostructured materials, gained increasing interest in the design of GDLs to overcome the above-described limitations, ensuring optimized gas diffusion, optimal water management and structural refinement [18, 31-32].

The present work proposes the development of a novel nanostructured-gas-diffusion-layer (nano-GDL) to improve the overall behavior of a-SCMFCs with the aim to obtain the best compromise among hydrophobicity and surface wettability properties of GDL. To overcome all the limitations associated to the unprecise use of PTFE, which can induce an incomplete wetting of the cathode electrode, novel nano-GDLs were prepared by the electrospinning process directly collecting on the same carbon-based electrode two different nanofiber mats. The electrohydrodynamic process promotes optimal interaction among the different layers, avoiding the need of a binder. The first layer (inner-layer) was made of cellulose nanofibers that play a crucial role to promote oxygen diffusion into SCMFC [29-30]. With the aim to improve the adhesion of this first nanostructured layer to the carbon backbone, in the present work, we propose to create carbonized patterns into the cellulose nanofibers by direct laser writing. To this purpose, the carbonized patterns were designed allowing the creation of graphene-like regions (i.e., Laser Induced Graphene) combined with un-treated cellulose nanofibers which played a key role ensuring the necessary hydrophilicity to improve water retention in proximity of the active catalytic sites, thus avoiding any decrease of proton conductivity of the electrolyte by dehydration [29-30]. The second layer (outward-layer) was based on polyvinyl-fluoride (PVDF) nanofibers with the main purpose to prevent the electrolyte

leakage, while allowing oxygen free to flow combined with a correct water removal from cathode electrode. **The design of new nano-GDL allowed exploiting all nanofibers intrinsic properties, such as high surface ratio to volume, high continuous porosity, and light weight, achieving thus a good oxygen diffusion in the proximity of the catalyst layer, ensuring optimal surface wettability, and thus favoring the direct ORR while preventing the water flooding in correspondence of catalyst layer.** We proposed the ideal catalyst layer for ORR, based onto Platinum on carbon [35], directly deposited on the inner side of carbon paper, on which both of two nanostructured layers were directly collected. To investigate the good performances of SCMFCs, achieved when nano-GDLs were employed, cathode electrodes with commercial gas diffusion layers, made of PTFE, were used for comparison. We demonstrated the capability of a-SCMFCs with nano-GDLs to achieve a maximum current density equal to  $(132.2 \pm 10.8) \text{ mA m}^{-2}$ , an order of magnitude higher than the one reached with commercial-PTFE, equal to  $(58.5 \pm 2.4) \text{ mA m}^{-2}$ . To confirm the extremely/excellent performances, provided by nano-GDLs, we propose an analysis of obtained results in terms of energy recovery, as already reported in our previous work [36]. In line with the trend obtained by analyzing the current densities, it is possible to state that nano-GDLs ensured the achievement of an energy recovery of  $60.83 \text{ mJ m}^{-3}$ , one order of magnitude higher than the value obtained by commercial-PTFE ( $3.92 \text{ mJ m}^{-3}$ ). All these latter results open the doors to the design of the whole nanostructured cathode electrode in SCMFCs. To achieve this goals, nitrogen-doped carbon nanofibers (N-CNFs) can be proposed as conductive carbon backbone, able to exploit simultaneously good electrocatalytic properties for ORR, as deeply defined in our previous work [11].

## 2. Materials and Methods

### 2.1 Gas Diffusion Layer package and nanofibers synthesis

Nanostructured GDLs were obtained by deposition of nanofibers mats directly onto carbon-based materials (Carbon Paper, purchased from Fuel Cell earth). To this purpose, electrospinning process (NANON 01A electrospinning apparatus MECC, LTD) was involved to design nano-GDLs, guaranteeing the ability to connect two different nanofibers' layers, without the use of a binder, suitable to connect all developed layer to the carbon backbone. **In this configuration, carbon paper pieces, cut in a square shape of  $(3 \times 3) \text{ cm}^2$ , were used as counter electrodes during the electrospinning process, leading thus to obtain cathode electrodes with the desirable geometric area for application in Microbial Fuel Cells.** Nano-GDLs were composed by two different layers. The first layer was based on cellulose nanofibers, obtained by implementing an hydrolyzation process of cellulose acetate nanofibers [37-38]. Indeed, cellulose acetate nanofibers were immersed for 1h in an ethanol-based solution containing 0.05M di NaOH. **To guarantee a successful carbonization process in ambient atmosphere, no subsequent washing is needed. In this way, it has been possible to perform the laser writing step under ambient conditions, directly obtaining the LIG patterns from the cellulose nanofibers. This experimental approach improves the adhesion of all nanostructured GDLs to the carbon backbone.** CO<sub>2</sub> Laser Writing (Pulsed CO<sub>2</sub> laser source, implementing by commercial Laser Scriber by Microla Optoelectronics S.r.l) was employed to occur the carbonization of cellulose nanofibers, as deeply investigated in the literature [37-38]. In particular, the great advantage of CO<sub>2</sub> laser writing was identified by the capability to create carbonized patterns onto nanofibers mats, following different and desirable paths. We proposed the possibility to perform the LIG step under ambient conditions, writing onto cellulose nanofibers carbonized patterns, which led to improve the adhesion of all nanostructured GDLs to the carbon backbone. The second layer was made of polyvinyl fluoride, PVDF-nanofibers, achieved by starting a polymeric solution of 2g of PVDF (Mw=150 kDa, Sigma Aldrich) dissolved in a mixture (1:1 v/v) of N-N Dimethylformamide (N-N DMF) and acetone. The deposition of PVDF

nanofibers is achieved to ensure the correct balance between hydrophilic properties and hydrophobic features, preventing possible leakage of electrolyte solution.

For both nanofibers' mats, the electrospinning parameters were an applied voltage of 26 kV, a working distance of 15cm and a flow rate of 0.5 mL h<sup>-1</sup>.

## 2.2 SCMFCs architecture and operation

The experiment was carried on using squared shape open-air cathode SCMFCs that we discussed in previous articles [10-11]. A 3D printer (OBJET 30) was used to fabricate the membrane-less cells, characterized by a single reaction chamber shared between anode and cathode. The two electrodes were kept at a fixed distance thanks to an intermediate septum, ensuring an inner volume of 12.5 mL. Both the electrodes have a squared shape, with a geometric surface area close to 5.76 cm<sup>2</sup>. They both were made of carbon paper (CP, from Fuel Cell Earth, USA). To ensure maximum anodic stability, all the anodes of the here proposed experiment have been obtained from a-SMFCs already running in our Labs [36], characterized by anodic biofilms made of mixed consortia. For what concerns the cathode electrodes, on the inner side of cathode electrode, standard platinum catalyst layer made of 0.5 mg cm<sup>-2</sup> of Pt/C (by Sigma Aldrich) and 5wt% of Nafion (Sigma Aldrich) was applied [34]. On the outer side of cathode electrode, with the main purpose to improve the triple phase boundary to ensure the direct ORR, and consequently increasing the overall devices' performance, three different GDLs were proposed and compared: i) the first one was made of a nanostructured GDL and was named nano-GDL: it consisted into 2 layers of nanofiber mats, the first one is made of hydrolyzed acetate nanofibers, on which a second layer of PVDF-nanofibers were deposited; ii) the second one, defined as nano-LIG GDL, was based on two different layers of nanofibers: a layer of cellulose nanofibers patterned by LIG and a PVDF-nanofibers layer; and iii) the third material was composed by a Polytetrafluoroethylene (PTFE) layer, and it is referred to as commercial-PTFE. A water-based solution containing 12 mM of sodium acetate was used as the electrolyte, with sodium acetate serving as the carbon-energy source. Ammonium chloride (5.8 mM) and phosphate buffer saline solution (PBS) [10-12] were added to the promote the metabolic activity of microorganisms. Titanium wires were employed for electrical contact and a multichannel data acquisition unit (Agilent 34972 A) was used to monitor the output voltage from the cells. Titanium wires were threaded through the polymeric frame, so that once the frame is correctly positioned inside the cathode compartment and exploiting the mechanical pressure obtained when closing the cell, an optimum electrical contact is ensured. An external load of 1k $\Omega$  was applied to each cell. Indirectly, through the first Ohmic Law, current values were defined. Moreover, a current density trend was obtained by dividing each current value for the geometric area of the electrode, equal to 5.76 cm<sup>2</sup>. All the devices were operated in fed-batch mode, thus ensuring the electrolyte replacement when the output voltage dropped to 0V. All the experiments were conducted in duplicate.

## 2.3 Characterizations and measurements

Field Emission Scanning Electron Microscopy (FESEM, Supra operating from 5 kV to 10 kV), is used to evaluate the morphological properties of nanostructured gas diffusion layer (GDL). Through the analysis of FESEM images allowed defining the preservation of nanostructures also after the LIG process, implementing to improve the adhesion of both nanofibers' layers, components of the new gas diffusion layer GDL. Moreover, to confirm the effective role of high continuous porosity onto diffusion of oxygen species inside the devices and onto the balance between water retaining and removing, FESEM images were analyzed with an imaging software (ImageJ).

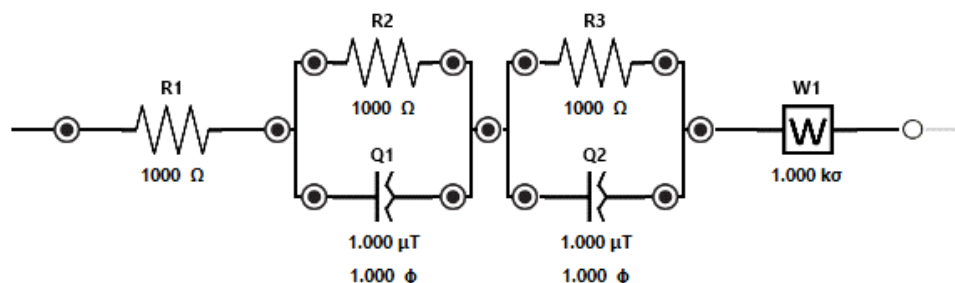
Final porosity of both samples, nano-LIG GDL and commercial-PTFE, were indirectly determined by dividing the volume occupied by nanofiber ( $V_{NF}$ ) or PTFE layer ( $V_{PTFE}$ ), respectively, by total volume ( $V_{tot}$ ).

$$\phi = \frac{(V_{NF} \text{ or } V_{PTFE})}{V_{TOT}}, \quad (1)$$

Furthermore, to confirm the effectiveness of image analysis performed on FESEM images, Brunauer–Emmett–Teller (BET, Micrometrics, ASAP 2020 Plus) measurements were implemented to define the specific surface area of nano-LIG GDLs, leading thus to evaluate the porosity distribution of the nanostructured layers.

To evaluate how nano-LIG GDL can affect SCMFCs performance, improving it with respect to the performance achieved with nano-GLD and commercial PTFE, Linear Sweep Voltammetry (LSV) characterizations were defined by using Palmsens potentiostat (Palmsens4, Netherlands). LSV characterizations were performed at the end of experimental study, ranging the voltage from open circuit to a short circuit at a rate of  $0.1 \text{ mV s}^{-1}$ . Electrochemical impedance spectroscopy (EIS), using a Palmsens potentiostat, were provided to define electrocatalytic features of cathodes. EIS analysis was performed applying an external fixed resistor of  $100 \Omega$  [12], using a sinusoidal signal with an amplitude of  $25 \text{ mV}$  and frequency spanning between  $150 \text{ kHz}$  and  $200 \text{ mHz}$ .

The equivalent circuit of Scheme 1 was used to fit the experimental data from EIS, in such a way to quantitatively evaluate the following electrical parameters: i)  $R1$ , i.e. the series resistance, accounts for electrolyte and wiring resistances; ii)  $R2$  and  $R3$  are associated to the resistances to charge transport inside the electrode and to the charge transfer at the electrode/electrolyte interface, respectively. Due to porous nature of cathode electrodes, constant phase elements,  $Q1$  and  $Q2$  are used to model the corresponding double layer capacitances [12].; and finally, iii) Warburg element was included to model low frequency feature, commonly corresponding to the species diffusion.



Scheme 1. Equivalent circuit used to fit the impedance spectra

### 3. Results and Discussion

#### 3.1. Morphological properties of nano-GDL and commercial-PTFE

Aiming to perform the LIG step in ambient conditions, to facilitate the fabrication process to scale it up, the main results was achieving by the definition of proper conditions for a graphitization avoiding the burning the material. Indeed, to ensure the carbonization of cellulose nanofibers, high temperatures must be reached, at which basically these synthetic polymers burned in the presence of oxygen. All these limitations demand the development of a polymeric nanofibers treatment capable of allowing and guaranteeing the carbonization of the nanofibers themselves **under ambient conditions, without the implementation of technical gases, such as argon or nitrogen, typically employed during the standard carbonization process** [36]. The obtained results highlighted how the deacetylation step, usually involved to transform the cellulose acetate nanofibers into cellulose nanofibers, if not followed by subsequent washing in deionized water, **resulted to be pivotal to ensure the carbonization of nanofibers under ambient conditions**. It was

possible to demonstrate that the presence of NaOH salts onto cellulose nanofibers resulted to have a key role to promote carbonization of cellulose nanofibers. As shown in **Figure 1a**, the presence of NaOH salt, decorating cellulose nanofibers mats, was confirmed by FESEM images, whereas on the contrary, NaOH was completely disappeared after the implementation of LIG process conducted in ambient condition, as represented in **Figure 1b**). Moreover, **Figure 1b**) allowed demonstrating the preservation of nanostructures also after the LIG process applied to create carbonized patterns onto nanofiber mats.

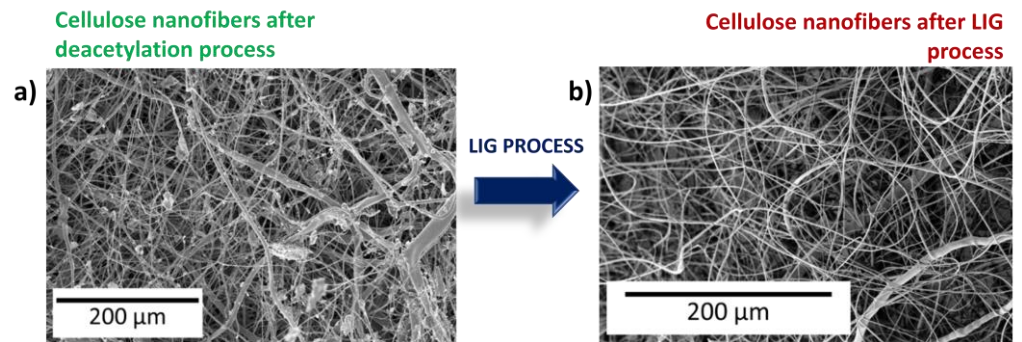


**Figure 1.** a) Morphological properties of cellulose nanofibers after deacetylation process, confirming the presence of NaOH salts onto nanofibers mats; b) morphological properties of carbonized cellulose nanofibers, guaranteeing the preservation of nanostructures also after the LIG process involved to create carbonized patterns onto nanofiber mats

This result can be explained by considering the hypothesis that the NaOH salts were able to sublime during the CO<sub>2</sub> laser writing process, ensuring the formation of an oxygen-free atmosphere during the process itself, leading thus the complete transformation of cellulose nanofibers into carbon-based nanofibers. With the main purpose to confirm the capability of CO<sub>2</sub> laser writing to transform into laser-induced Graphene (LIG)- nanofibers the initial cellulose nanofibers, Raman characterization was employed. As reported in **Figure 2**, it is possible to detect an achieved graphitization of material as evidenced by the presence of the G peak at about 1580 cm<sup>-1</sup>. The graphitization is certainly partial, and the presence of a pronounced 'neck' between the G peak and the D peak (at about 1350 cm<sup>-1</sup>) indicates the presence of groups of various kinds bound to the graphitic lattice. These groups can be defined as oxygen-containing functional groups due to the partial graphitization of the starting cellulose nanofibers [37]. For what concerned the 2D band peak, this peak is not detectable due to the low degree of graphitization, leading thus to exclude this part of spectrum, because it does not provide any further information.

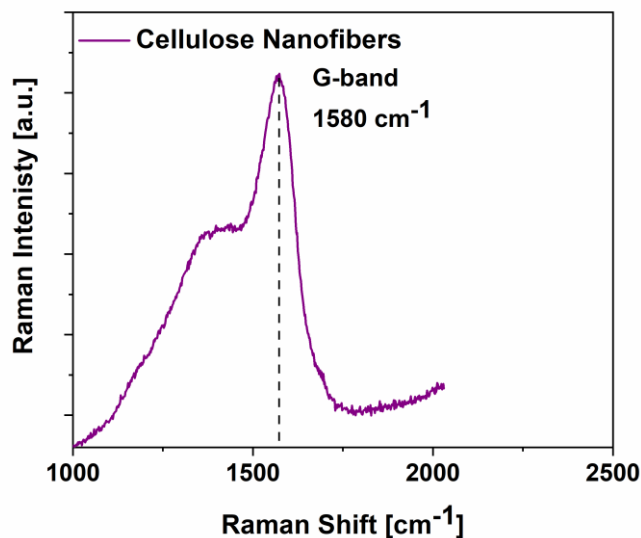


**Figure 2.** Raman spectrum of carbonized patterns created onto cellulose nanofibers thanks to the implementation of CO<sub>2</sub> laser writing. The presence of G-band at 1580 cm<sup>-1</sup> confirmed the achieved graphitization of nanofibers, that remain partial, highlighting the presence of oxygen-containing functional groups as confirmed by the 'neck' between the G peak and the D peak (at about 1350 cm<sup>-1</sup>)

Moreover, the morphological properties of the whole nano-LIG GDLs, obtained after the deposition of PVDF-nanofiber layers on the cellulose nanofibers, previously carbonized through CO<sub>2</sub> laser writing process, were investigated and reported in Figure 3a), highlighting thus the pore distribution in these samples. Indeed Nano-LIG GDL are characterized by pores with dimensions in the range of few micrometers, leading thus to exhibit a higher surface area to volume ratio than the one obtained with commercial gas diffusion layers, commercial-PTFE (see Figure 3b). The ImageJ software allowed indirectly evaluating the porosity distribution into Nano-LIG GDL, comparing it with the one achieved with commercial-PTFE. To this purpose, the porosity distribution of all samples was determined by applying Equation 1. Figure 3c) allowed confirming that the porosity distribution of Nano-LIG GDL, close to 77%, results to be higher than the one when commercial-PTFE was applied (equal to 25%). High porosity distribution values are in line with the results achieved by determining specific surface area of whole nano-LIG GDLs by implementing Brunauer–Emmett–Teller (BET) measurements. Nano-LIG GDLs showed a specific surface area of 18.94 ± 0.05 m<sup>2</sup>/g. Moreover, from BET measurements, it is possible to define the pores distribution inside the whole nanostructured layers. Nano-LIG GDLs showed pores dimension in the range from 2nm to 10 nm, leading thus to define that Nano-LIG GDLs is a micro and mesoporous material. High continuous porosity showed in Figure 3c), greater than the one achieved by commercial-PTFE, can positively affect the diffusion of oxygen from outside towards the catalytic active sites, leading thus to improve the triple phase boundary. These intrinsic properties of nanofibers with particular attention on their high continuous porosity can play a pivotal role into the enhancement of oxygen diffusion in proximity of triple contact zone, ensuring thus a better oxygen transport in proximity of catalytic active sites.



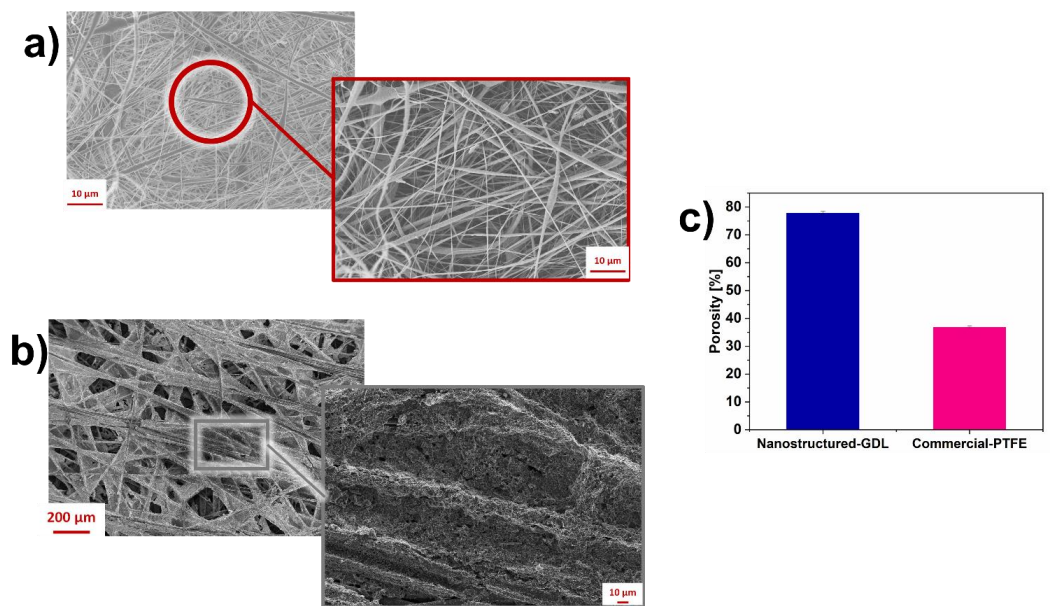


**Figure 3.** a) Morphological properties of nanostructured-LIG GDLs, confirming high porosity of samples, as highlighted from higher magnification, underlined by red box; b) Morphological properties of commercial-PTFE; c) Evaluation of porosity distribution of nanostructured-LIG GDLs compared with the one reached with commercial-PTFE.

### 3.2 SCMFCs performance

As previously described, anodes electrodes, on which a microorganisms proliferation occurred were obtained by preceding experiments [36]. For all cathode electrodes platinum is involved as catalyst, while nano-LIG GDL, nano-GDL and commercial-PTFE were compared, to evaluate how all the properties of both nano-GDLs can affect the overall performance of SCMFCs. **Figure 4** represents the current density trends over time. Nano-LIG GDL reached a maximum current density equal to  $(151.2 \pm 15.5) \text{ mA m}^{-2}$ , which is double of the one reached with Nano-GDL, confirming how the presence of conductive patterns played a pivotal role to ensure the design of a better performing Gas Diffusion Layer. Moreover, Figure 4 also highlighted that nanostructured arrangement of Gas diffusion Layers allowed achieving improved overall SCMFCs performance, if compared with commercial-PTFE (maximum current density close to  $(58.5 \pm 2.4) \text{ mA m}^{-2}$ ), used as reference material. Since the anodes electrodes resulted to be formally identical for all devices, it is possible to attribute the different power production of SCMFCs directly to the development of diverse nano-GDLs onto cathode electrodes.

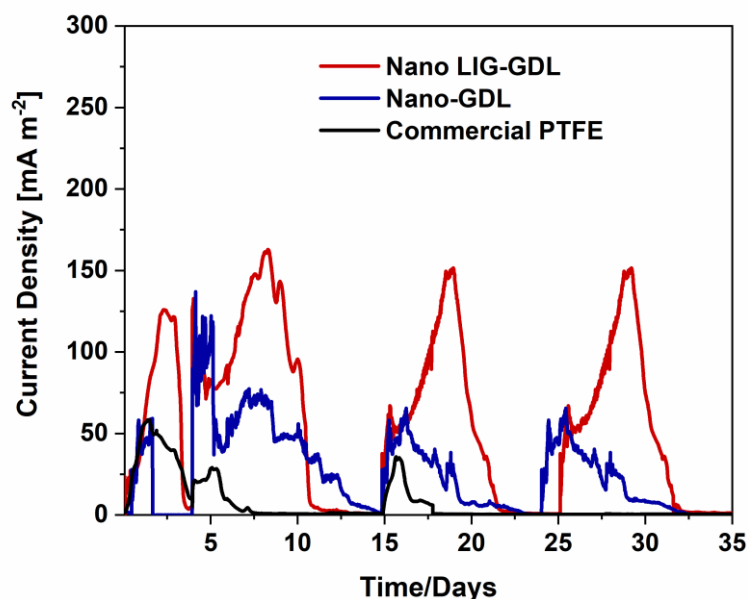


**Figure 4.** Comparison of average current density trend of SCMFCs with nano-GDL and nano-LIG GDL compared with the one achieved by SCMFCs made of commercial-PTFE

This latter result allowed confirming the key role of nano-LIG GDL with a great interest onto the presence of conductive patterns, creating through the CO<sub>2</sub> laser writing, able to further improve overall SCMFCs' performance. Indeed, the presence of conductive patterns could improve the contact between the whole nanostructured GDL and the carbon backbone, allowing the enhancement of the triple contact zone, oxygen diffusion in proximity of catalytic active sites and, at the same time, thanks to the presence of hydrophilic cellulose-NFs layers, the exceed water removal from catalytic sites. The combination of these features affects the electrocatalytic efficiency of electrode toward direct-ORR, reflecting thus onto the augmented overall SCMFCs' performance. In line with the obtained results, we performed LSV and electrochemical characterizations onto SCMFCs that showed nano-GDL, nano-LIG GDL and commercial-PTFE.

Both of SCMFCs devices reach a similar open circuit voltage (OCV) close to 0.4V, while SCMFCs with nano-LIG GDL achieved a higher short circuit current (close to 262±5 mA m<sup>-2</sup>) that the one obtained with commercial-PTFE (176.4±3.2 mA m<sup>-2</sup>). Since nano-LIG GDL can affect and favor the direct ORR, ensuring the best oxygen diffusion into SCMFCs, the variation of total cathodic resistance over time was investigated through EIS. Typical Nyquist plots are represented in **Figure 5b**), comparing nano-LIG GDL and commercial one. The curves obtained by fitting procedure are overlaid on the experimental data (see **Figure5b**). **Table 1**, on the contrary, summarized all resistance values.

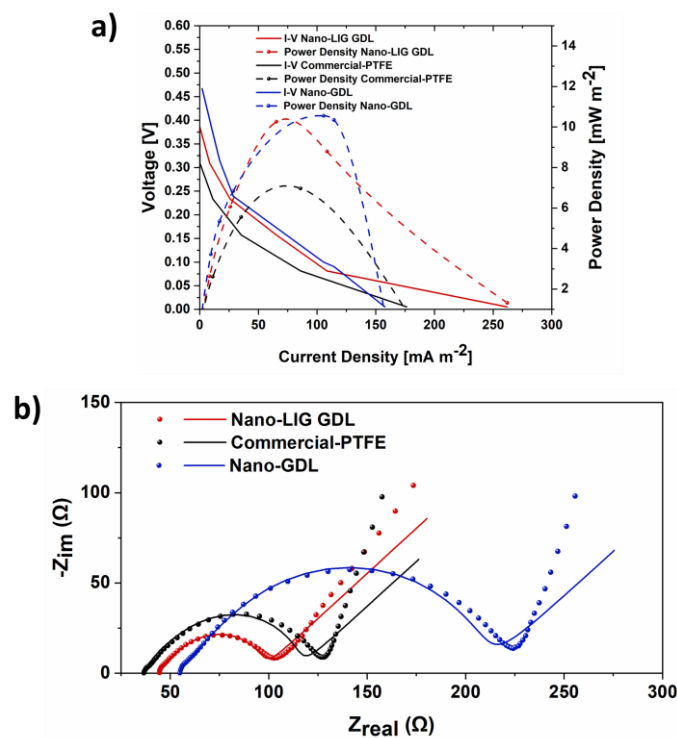


**Figure 5.** a) Polarization curves obtained by LSV characterization. Potential vs. current density curves (left axis, straight lines) and power density vs. current density (right axis, dash lines) curves of all SCMFCs. b) Typical impedance spectra of nano-LIG GDL (red dot and line), nano-LIG (blue dot and line) and commercial-PTFE (black dot and line).

As highlighted in Figure 5b), all SCMFCs show a similar value of series resistance  $R_1$ , independently of cathode electrodes. This is to be expected, since electrolyte, wires and electrical connection are identical for all SCMFCs. Moreover, the lower is the charge transfer at the electrode/electrolyte interface  $R_3$ , higher is the capacity of cathode electrode to ensure a faster electrons flow. This result demonstrates the effectiveness of nano-LIG GDL to ensure an enhancement of oxygen diffusion, improving consequently the occurring of direct-ORR and the overall SCMFCs performance. A similar trend is observed for the transport resistance  $R_2$ , which is visible in the high-frequency smaller arc sketched in Figure 5b).

A lower  $R_2$  defines an increasing of electrode transport properties and since all other aspects of cathode electrodes are the same, it is possible to confirm how nano-GDL results to be more efficient in carrying out ORR.

**Table 1.** Typical resistance values ( $R_1$ ,  $R_2$  and  $R_3$ ) calculated from the fitting procedure on Electrochemical Impedance Spectroscopy (EIS) data. For each parameter, the maximum variation observed between three nominally identical Microbial Fuel Cells (MFCs) was 10%.

Cathode electrodes	$R_1$ [Ω]	$R_2$ [Ω]	$R_3$ [Ω]
Nano-LIG GDL	44.3	12.04	38.4
Nano-GDL	54.17	24.69	128.8
Commercial-PTFE	36.9	25.7	50.5

Moreover, in line with all obtained results, the analysis performed in terms of energy recovery parameter, defined as ratio of generated power integral and the internal volume of devices, allow evaluating the overall SCMFC performance. SCMFCs with a nano-LIG

GDL showed an energy recovery equal to 60.83 mJ m<sup>-3</sup>, which was one order of magnitude higher than the one obtained with commercial-PTFE, close to 3.92 mJ m<sup>-3</sup>

#### 4. Conclusion

In the present work, nano-LIG GDL was designed as new gas diffusion layer to improve the oxygen diffusion inside SCMFCs, exploiting the intrinsic properties of nanofibers, such as high porosity, high surface area to volume ratio and light weight. Moreover, through electrospinning process, nanofiber mats were directly collected on carbon-based materials, used as cathode electrodes, without the necessity of binder to bond GDL with the carbon backbone. Morphological analysis gave evidence of a higher porosity obtained with nano-GDL, than that reached using commercial-PTFE.

All obtained results demonstrate that nano-LIG GDLs are effective in improving a-SCMFCs performance, showing a maximum current density value that doubles the one obtained using standard PTFE. Since the changes introduced among the cathodes used in this work are referred to the new nano-LIG GDLs, it is possible to confirm that the observed improvement is related to use of nanostructured materials for GDL. All the obtained results demonstrate the effectiveness of nano-LIG GDL to ensure an enhancement of oxygen diffusion, consequently enhancing the direct-ORR and thus the final performance a-SCMFCs.

**Author Contributions:** Conceptualization, G.M and M.Q.; methodology, G.M. and M.Q.; validation, formal analysis and investigation, G.M.; resources, M.Q and C.F.P.; data curation, G.M.; writing—original draft preparation, G.M.; writing—review and editing, T.S., M.Q and C.F.P.; visualization, G.M and M.Q; supervision, project administration and funding acquisition, M.Q and C.F.P. All authors have read and agreed to the published version of the manuscript.

**Funding:** Tommaso Serra's Ph.D. grant was funded by National Operational Program (PON) Research and Innovation 2014–2020 (CCI 2014IT16M2OP005), resources FSE REACT-EU, Action IV.5 "Dottorati su tematiche Green".

This publication is part of the project NODES- which has received funding from the MUR – M4C2 1.5 of PNRR funded by the European Union – Next Generation EU (Grant agreement no. ECS00000036).

This study was carried out within the MICS (Made in Italy–Circular and Sustainable) Extended Partnership and received funding from the European Union Next-Generation EU (PIANO NAZIONALE DI RIPRESA E RESILIENZA (PNRR) –MISSIONE 4 COMPONENTE 2, INVESTIMENTO 1.3 –D.D. 1551.11-10-2022, PE00000004). This manuscript reflects only the authors' views and opinions, neither the European Union nor the European Commission can be considered responsible for them.

**Data Availability Statement:** No Data availability statement.

**Acknowledgments:**

**Conflicts of Interest:** The authors declare no conflict of interest.

#### References

1. B. Walsh, P. Ciais, I.A. Janssensz, J. Penuelas, J. K. Riahi, F. Rydza, D.P. Van Vuuren, M. Obersteiner. Pathways for balancing CO<sub>2</sub> emissions and sinks. *Nature Communication* **2017**, *8*, 14856–68.
2. Liu B., Li B. Single chamber microbial fuel cells (SCMFCs) treating wastewater containing methanol. *International Journal of Hydrogen Energy* **2014**, *39*, 2340–44 154–196.
3. Cistiani P., Trasatti S.P. In Field Applications of Single Chamber Membraneless Microbial Fuel Cells (SCMFCs) for Wastewater Treatment, Metal Reduction and Nutrients Removal. **2014 Meet. Abstr.** MA2014-02 2283. DOI: 10.1149/MA2014-02/50/2283
4. Logrono W., Perez m., Urquizo G., Kadier A., Echeverria M., Recalde C., Rakhely G. Single chamber microbial fuel cell (SCMFC) with a cathodic microalgal biofilm: A preliminary assessment of the generation of bioelectricity and biodegradation of real dye textile wastewater. *Chemosphere* **2017**, *176*, 378–388
5. Tanikkul P., Pisutpaisal N. Membrane-less MFC based biosensor for monitoring wastewater quality. *International Journal of Hydrogen Energy* **2018**; *43*: 483–489.

6. Quaglio M., Massaglia G., Vasile N., Margaria V., Chiodoni A., Salvador G.P., Marasso S.L., Cocuzza M., Saracco G., Pirri C.F. A fluid dynamics perspective on material selection in microbial fuel cell-based biosensors. *International Journal of Hydrogen Energy* **2019**; *44*: 4533-4542 413-415
7. Di Lorenzo M., Curtis T.P., Head I.M., Velasquez-Orta S.B; Scott K. A single chamber packed bed microbial fuel cell biosensor for measuring organic content of wastewater. *Water Sci. Technol.* **2009**; *60*:2879-2887 416-417
8. Logan, B.E.; Rabaey, K. Conversion of wastes into bioelectricity and chemicals by using microbial electrochemical technologies *Science* **2012**, *337*, 686-690[9] Logan, B.E. Microbial Fuel Cells, New York: John Wiley & Sons; 2008 418-419
9. Logan, B.E.; Hamelers, B.; Rozendal, R.; Schroder, U.; Keller, J.; Freguia, S.; Aelterman, P.; Verstraete, W.; Rabaey, K. Microbial fuel cells: methodology and technology. *Environmental Science and Technology* **2006**, *40*, 5181-92 420-421
10. Babauta, J.; Renslow, R.; Lewandowski, Z.; Beyenal, H. Electrochemically active biofilms: facts and fiction. A review *Biofouling* **2012**, *28*, 789-812 422-423
11. Harnisch, F.; Aulenta, F.; Schroeder, U. Comprehensive Biotechnology 2nd ed; Elsevier: Amsterdam, 2011, p. 644-659 424
12. Dange P., Savla N., Pandit S., Bobba R., Jung S.P., Gupta P.K., Sahni M., Prasad R. A Comprehensive Review on Oxygen Reduction Reaction in Microbial Fuel Cells. *Journal of Renewable Materials* **2022**; *10*:3-34. DOI: 10.32604/jrm.2022.015806 425-426
13. Liew K.B., Daud W.R.W; Ghasemi M., Leong J.X. Lim S.S. Ismail M. Non-Pt catalyst as oxygen reduction reaction in microbial fuel cells: A review. *International Journal of Hydrogen Energy*. **2014**; *38*:4870-4883 427-428
14. Chandrasekhar K. Chapter 3.5 - Effective and Nonprecious Cathode Catalysts for Oxygen Reduction Reaction in Microbial Fuel Cells. Microbial Electrochemical Technology Sustainable Platform for Fuels, Chemicals and Remediation Biomass, Biofuels and Biochemicals (2019), Amsterdam: Elsevier; 2019 (Pages 485-501) 429-431
15. Chaturvedi A., Kundu P.P. Enhancing sustainable bioelectricity generation using facile synthesis of nanostructures of bimetallic Co-Ni at the combined support of halloysite nanotubes and reduced graphene oxide as novel oxygen reduction reaction electrocatalyst in single-chambered microbial fuel cells. *International Journal of Hydrogen Energy*. **2022**; *47*: 29413-29429 432-433
16. Sciarria T.P., Costa De Olyveira m.A., Mecheri B., D'ePifanio A., Goldfarb J.L, Adani F. Metal-free activated biochar as an oxygen reduction reaction catalyst in single chamber microbial fuel cells. *Journal of Power Sources* **2020**; *462*:228183. DOI: 10.1016/j.jpowsour.2020.228183 434-436
17. Cindrella L., Kannan A.M., Lin J.F., Saminathan K., Ho Y., Lin C.W, Wertz J. Gas diffusion layer for proton exchange membrane fuel cells – A review. *Journal of Power Sources*, **2009**; *194*:146-160 437-439
18. Wang Y.C, Huang W., Wan L.Y., Yang J., Xie R.J., Zheng Y.P, Tan Y.Z., Wang Y.S, Zaghib K., Zheng L.R., Sun S.H., Zou Z.Y., Sun S.G. Identification of the active triple-phase boundary of a non-Pt catalyst layer in fuel cells. *Sci. Adv.* **2022**; *8*: eadd8873. DOI: 10.1126/sciadv.add8873 440-442
19. Wang Y., Pang Y., Xu H., Martinez A., Chen K.S. PEM Fuel cell and electrolysis cell technologies and hydrogen infrastructure development – a review. *Energy Environ. Sci.*, **2022**, *15*, 2288. DOI: 10.1039/d2ee00790h 443-444
20. Garapati M.S., Nechiyil D., Jouliè S., Bacsá R.R., Sundara R., Bacsá W. Proton-Conducting Polymer Wrapped Cathode Catalyst for Enhancing Triple-Phase Boundaries in Proton Exchange Membrane Fuel Cells. *ACS Appl. Energy Mater.* **2022**, *5*, 627–638 445-446
21. Santoro C., Agrios A., Pasaogullari U., Li B. Effects of gas diffusion layer (GDL) and micro porous layer (MPL) on cathode performance in microbial fuel cells (MFCs). *International Journal of Hydrogen Energy*. **2011**; *36*: 13096-13104 447-449
22. Jordan L.R, Shukla A.K., Behrsing T., Avery N.R., Muddle B.C., Forsyth M., Diffusion layer parameters influencing optimal fuel cell performance. *J. Appl. Electrochem.* **2000**, *30* 641-646. 450-451
23. Neergat M., Shukla A.K., Effect of diffusion-layer morphology on the performance of solid-polymer-electrolyte direct methanol fuel cells. *J. Power Sources* **2002**, *104* 289-294. 452-453
24. Choi S. Wan Do H., Jin D., Kim S., Lee J., Soon A., Moon J., Shim W. Revisiting the Role of the Triple-Phase Boundary in Promoting the Oxygen Reduction Reaction in Aluminum–Air Batteries. *Advanced functional Materials* **2021**; *31*:2101720. DOI: 10.1002/adfm.202101720. 454-456
25. Mathas M.F., Roth J., Fleming J., Lehnert W., Vielstich W., Gasteiger H.A. et al. editors. HandBOK of Fuel Cells-Fundamentals, Technology and Applications. Vol.3. New York; John Wiley & Sons; 2003 (Chapter 42). 457-458
26. Li H, Tang Y, Wang Z, Shi Z, Wu S, Song D, et al. A review of water flooding issues in the proton exchange membrane fuel cell. *Journal of Power Sources* **2008**; *178*: 103-117. 459-460
27. Pasaogullari U, Wang CY. Two-phase transport and the role of micro-porous layer in polymer electrolyte fuel cells. *Electrochimica Acta* **2004**; *49*:4359-4569. 461-462
28. Gostick JT, Fowler MW, Ioannidis MA, Pritzker MD, Volfkovich YM, Sakars A. Capillary pressure and hydrophilic porosity in gas diffusion layers for polymer electrolyte fuel cells. *Journal of Power Sources* **2006**; *156*:375. 463-464
29. Guerrini E., Grattieri M., Faggianelli A., Cristiani P., Trasatti S. PTFE effect on the electrocatalysis of the oxygen reduction reaction in membraneless microbial fuel cells. *Bioelectrochemistry*. **2015**; *106*: 240-247 465-466
30. Y.W. Chen-Yang, T.F. Hung, J. Huang, F.L. Yang, Novel single-layer gas diffusion layer based on PTFE/carbon black composite for proton exchange membrane fuel cell. *J. Power Sources*. **2007**; *173*: 183–188. 467-468
31. V. Kamavaram, V. Veedu, A.M. Kannan, Synthesis and characterization of platinum nanoparticles on in situ grown carbon nanotubes based carbon paper for proton exchange membrane fuel cell cathode. *J. Power Sources* **2009**: 188:51–56. 469-470

- 
32. Hirakata S., Hara M., Kakinuma K., Uchida M., Tryk D.A. Uchida H., Watanabe M. Investigation of the effect of a hydrophilic layer in the gas diffusion layer of a polymer electrolyte membrane fuel cell on the cell performance and cold start behaviour. I. **2014**; 120: 247-247 471  
472  
473
  33. T. Kitahara, H. Nakajima, M. Inamoto, M. Morishita, Novel hydrophilic double microporous layer coated gas diffusion layer to enhance performance of polymer electrolyte fuel cells under both low and high humidity, *Journal of Power Sources* **2013**; 234: 129. 474  
475  
476
  34. Oh S, Min B, Logan BE. Cathode performance as a factor in electricity generation in microbial fuel cells. *Environmental Science Technology* **2004**; 38: 4900-4904 477  
478
  35. Massaglia G., Frascella F., Chiadò A., Sacco A., Marasso S.L., Cocuzza M., Pirri C.F, Quaglio M. Electrospun Nanofibers: from Food to Energy by Engineered Electrodes in Microbial Fuel Cells. *Nanomaterials* **2020**; 10: 523. DOI: 10.3390/nano10030523 479  
480
  36. Massaglia G., Margaria V., Sacco A., Castellino M., Chiodoni A., Pirri C.F., Quaglio M. N-doped carbon nanofibers as catalyst layer at cathode in single chamber Microbial Fuel Cells. *IJHE* **2019** 44: 4442-4449 481  
482
  37. Lee, S.; Jeon, S. Laser-Induced Graphitization of Cellulose Nanofiber Substrates under Ambient Conditions. *ACS Sustain. Chem. Eng.* **2019**, 7, 2270–2275, doi:10.1021/acssuschemeng.8b04955 483  
484
  38. Dizge N., Shaulsky E., Karanikola V. Electrospun cellulose nanofibers for superhydrophobic and oleophobic membranes. *Journal of Membrane Science* **2019**, 590, 117271 485  
486

**Disclaimer/Publisher's Note:** The statements, opinions and data contained in all publications are solely those of the individual author(s) and contributor(s) and not of MDPI and/or the editor(s). MDPI and/or the editor(s) disclaim responsibility for any injury to people or property resulting from any ideas, methods, instructions or products referred to in the content. 487  
488  
489